MJFAS MALAYSIAN JOURNAL OF FUNDAMENTAL AND APPLIED SCIENCES
PRINT ISSN: 2289-5981 | ONLINE ISSN: 2289-599X

RESEARCH ARTICLE

Highly efficient zinc oxide-carbon nitride composite photocatalysts for degradation of phenol under UV and visible light irradiation

Faisal Hussin [a], Hendrik Oktendy Lintang [b, c, d], Siew Ling Lee [a, b], Leny Yuliati [b, c, d,*]

[a] *Department of Chemistry, Faculty of Science, Universiti Teknologi Malaysia, 81310 UTM Johor Bahru, Johor, Malaysia*
[b] *Centre for Sustainable Nanomaterials, Ibnu Sina Institute for Scientific and Industrial Research, Universiti Teknologi Malaysia, 81310 UTM Johor Bahru, Johor, Malaysia*
[c] *Ma Chung Research Center for Photosynthetic Pigments, Universitas Ma Chung, Villa Puncak Tidar N-01, Malang 65151, East Java, Indonesia*
[d] *Department of Chemistry, Faculty of Science and Technology, Universitas Ma Chung, Villa Puncak Tidar N-01, Malang 65151, East Java, Indonesia*

* *Corresponding author: leny.yuliati@machung.ac.id*

Article history
Submitted 12 January 2018
Revised 4 February 2018
Accepted 22 February 2018
Published Online 30 April 2018

Graphical abstract

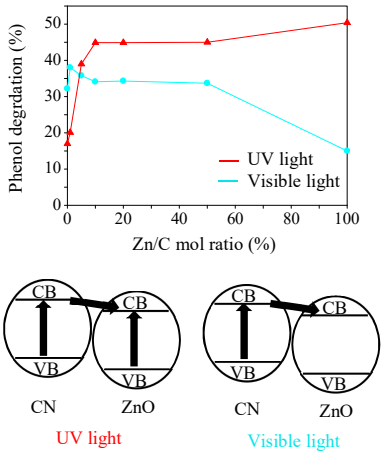

Abstract

In order to utilize solar light in an efficient way, a good photocatalyst shall absorb both UV and visible light. In this study, a series of composite photocatalyst consisting of zinc oxide (ZnO) and carbon nitride (CN) was successfully prepared through a physical mixing method. The ZnO is an ultraviolet (UV)-based photocatalyst, while the CN is known as a visible light-driven photocatalyst. The effect of zinc to carbon mol ratio (Zn/C) towards the properties and photocatalytic activities was investigated. X-ray diffraction (XRD) patterns revealed that the prepared ZnO-CN composite photocatalysts composed of wurtzite ZnO and graphitic CN. The presence of ZnO and CN made the composites have absorption at both UV and visible region, suggesting the potential application as photocatalysts under both UV and visible light. Fluorescence studies revealed that all ZnO-CN composites showed emission peaks at 445 and 460 nm when excited at 273 nm, but with lower intensity as compared to those of the CN. The lower emission intensity suggested the role of ZnO to reduce the charge recombination and improve the charge separation on the CN. The ZnO-CN composites were further evaluated for photocatalytic degradation of phenol. The amount of degraded phenol was determined by a gas chromatography, in which a flame ionization detector was used in this study (GC-FID). The composite photocatalyst with an optimum content of 1% Zn/C gave almost 1.15 times higher activity than the CN under visible light irradiation. On the other hand, the composite photocatalyst with an optimum content of 10% Zn/C showed 2.6 times higher activity than the CN under UV light. The improved photocatalytic efficiency on the ZnO-CN composite photocatalysts was caused by the synergic effect between ZnO and CN. The ZnO would boost the separation efficiency of photogenerated electrons on the CN, while the CN would enable ZnO to absorb visible light region as the ZnO-CN composites.

Keywords: carbon nitride, phenol, physical mixing, synergic effect, zinc oxide

INTRODUCTION

Zinc oxide (ZnO) with tremendous unique advantages is generally used in various practical applications, for instances in the electronic and optoelectronic (Djurišić *et al*., 2010; Logothetidis *et al*., 2008), catalysis (Lorenz *et al*., 2013; Sabbhagan and Ghalaei, 2014), biomedicine and biosensing (Ansari *et al*., 2011a; Arya *et al*., 2012), energy storage (Cauda *et al*., 2014) and solar cell (Cauda *et al*., 2014; Huang *et al*., 2011; Li *et al*., 2012). ZnO has been recognized to show an exceptional potential ability in the photocatalysis due to its unique properties of having a wide band gap in the UV range of 3.37 eV, high chemical inertness, immense quantum efficiency, low toxicity, strong oxidation ability, excellent redox potential, tunable morphology, high abundance and easily soluble in organic solvents (Behnajady *et al*., 2006; Chen *et al*., 2008a; Chen *et al*., 2014; Chekir *et al*., 2016).

Even though ZnO showed great activities in the photocatalytic remediation of pollutants and organic dyes, it could only absorb light in the UV region due to its large band gap. An enormous amount of energy is needed to activate ZnO as a photocatalyst since UV light comprises only 5% portion of the solar spectrum. Therefore, modification of ZnO to extend its absorption to the visible light region must be performed. Several attempts to obtain ZnO with visible light property have been developed, such as by tailoring and modification of the surface property of ZnO with dopants (Chen *et al*., 2008b; Kong *et al*., 2009; Zhang *et al*., 2012), dye sensitization (Saikia *et al*., 2015; Velmurugan and Swaminathan, 2011; Yang and Chan, 2009), polymers (Olad and Nosrati, 2012; Qiu *et al*., 2008), and surface passivation (Li *et al*., 2009). Semiconductor coupling of ZnO with other narrow band gaps semiconductors such as CuO (Saravanan *et al*., 2011), CdO (Saravanan *et al*., 2013) and BiOI (Jiang *et al*., 2011) offered promising results as compared to other approaches mentioned above since it provided a synergic effect which induced adequate charge separations for the improvement of the photostability especially to tackle the problem of ZnO photocorrosion.

Recently, research on the polymeric carbon nitride (CN) as a free-metal semiconductor and visible light-driven photocatalyst is particularly in interest due to its great properties, such as high photostability, large surface area, good response to the visible light absorption up to *ca*. 470 nm, and its abundance (Ansari *et al*., 2011b). However, bare CN alone suffered electron-hole recombinations,

which limited its performances for various photocatalytic applications. In order to cover up the weaknesses of the CN, composites consisting of CN with other active semiconductor have been proposed. For instance, TiO_2-CN composite showed two times higher performance than bulk CN for hydrogen evolution under visible light irradiation (Yan and Yang, 2011). Another composite, the CdS-CN, showed an exceptional activity compared to only individual CN or CdS for decomposition of methyl orange and 4-aminobenzoic acid (Fu *et al*., 2013). A composite consisting of Ga_2O_3 and CN has been also reported to give better activity for oxidation of cyclohexane (Lee *et al.*, 2015).

Phenol was used as the model of organic pollutant in this work. Previous studies showed that both ZnO (Hussin *et al.*, 2015) and CN (Lee *et al.*, 2012) acted as good photocatalysts for phenol degradation under UV and visible light irradiation, respectively. The interactions between phenol and ZnO (Hussin *et al.*, 2015) as well as between phenol and the CN (Yuliati *et al.*, 2017) were also reported. In order to improve visible light absorption of ZnO as well as to suppress the electron-hole recombinations of CN during exposure of visible light irradiation, a composite of ZnO-CN has been recently developed by an impregnation method (Hussin *et al.*, 2016). It has been reported that CN has conduction and valence bands at -0.73 and 1.97 eV vs NHE, respectively (Zhang *et al*., 2015), while the bands of ZnO are close to -0.25 and 3.0 eV vs NHE (Grätzel, 2001). Owing to the suitable band position, the electron charge transfer could occur from the conduction band of the CN to that of the ZnO. In this study, a composite consisting of ZnO and CN was developed by a simpler method, which was a physical mixing method. The results suggested that the composite photocatalyst prepared by the physical mixing method showed a comparable level of activity to those prepared by the impregnation method.

EXPERIMENTAL

Materials

The precursor materials for ZnO and CN were zinc acetate dihydrate ($Zn(CH_3COO)_2.2H_2O$, 99.5%, QRëC) and urea ($CO(NH_2)_2$, 99.5%, Sigma), respectively. The chemicals used for the preparation of ZnO and CN were commercial chemicals without further treatments or purifications.

Synthesis of ZnO

For the typical synthesis of ZnO, $Zn(CH_3COO)_2.2H_2O$ was calcined at 550 °C for 4 h. The heating rate was set at 2.2 °C min^{-1}. (Hussin *et al.*, 2015). The resulted solid was white in color.

Synthesis of CN

Urea as a source of carbon and nitrogen was calcined under the similar condition to the synthesis of ZnO. The calcination process was carried out at 550 °C for 4 h and the heating rate was fixed at 2.2 °C min^{-1} (Lee *et al.*, 2012). The resulting solid was yellow in color.

Synthesis of ZnO-CN (*x*)

Various ZnO-CN (*x*) samples were prepared by a physical mixing method with Zn/C ratios are 1, 5, 10, 20, and 50 mol%. The samples were labeled as ZnO-CN (*x*) with *x* represents the ratio of Zn to C (Zn/C) in mol%. In order to synthesize ZnO-CN (*1*), the ZnO (0.0266 g) was physically mixed with the CN (1 g). The color appearance of the obtained solid of all ZnO-CN (*x*) is shown in Fig. 1.

Photocatalyst characterizations

In order to clarify the structure of the prepared ZnO-CN composite photocatalysts, the X-ray diffraction (XRD) patterns of the samples were recorded on a diffractometer (Bruker, D8 Advance) with the 2θ range of 10-75° and scan step rate of 0.05° s^{-1}. Fourier transform infrared (FTIR) spectra were measured on a spectrophotometer (Nicolet iS50 Thermo Scientific) to investigate the functional groups of the composites. The capability of the composites to absorb UV and visible region was studied by a Shimadzu UV-2600. In order to obtain the specific surface area of the samples, Brunaeur-Emmett-Teller (BET) equation was used. The nitrogen adsorption data were obtained on a Quantachrome NOVAtouch LX4. Before each measurement, degassing process at 150 °C for 2 h was conducted to clean and remove any adsorbed gases on the surface of the sample. The emission spectra of the samples were obtained at room temperature on a fluorescence spectroscopy (JASCO FP-8500), using the excitation wavelength of the CN, which was at a wavelength of 273 nm corresponded for N=C groups (Alim *et al.*, 2015; Jasman *et al.*, 2017a; Jasman *et al.*, 2017b; Sam *et al*., 2014).

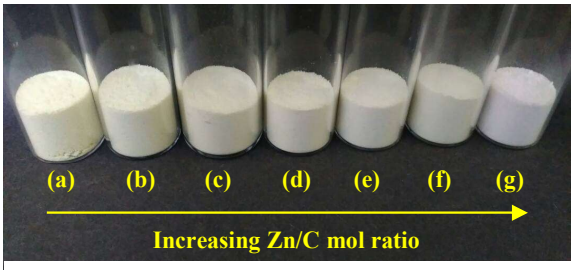

Fig. 1 Color appearance of CN, ZnO-CN (*x*) composites, and ZnO. From left to right: (a) CN, (b) ZnO-CN (*1*), (c) ZnO-CN (*5*), ZnO-CN (*10*), (e) ZnO-CN (*20*), (f) ZnO-CN (*50*) and (g) ZnO.

Photocatalytic activity testing

The photocatalytic degradation of phenol was conducted at room temperature. The photocatalyst (50 mg) was dispersed in 100 mL of jacketed-beaker containing phenol solution using acetonitrile as solvent (50 ppm, 50 mL). Prior to the photocatalytic reaction, the solution was stirred for 30 min in the dark to let the adsorption process occur. The reaction was then carried out for 5 h under UV light (8 W, light wavelength was centered at 254 nm with an intensity of 0.4 mW cm^{-2}) or visible light irradiation (150 W, light wavelength was more than 400 nm with an intensity of 100,000 lux). After each photocatalytic reaction, the photocatalyst was separated from the solution. The remaining phenol in the solution was sent for analysis by using a gas chromatography (GC, Agilent 7820A). The detector type was flame ionization detector (FID) and the column used was HP-5 (30 m × 320 µm × 0.5 µm). The activity of the photocatalyst was associated with the percentage of phenol degradation, which was determined by the following equation.

$$\text{Phenol degradation (\%)} = \frac{C_o - C}{C_o} \times 100\%$$

where C_0 and C showed the initial and final concentrations of phenol in solution before and after the photocatalytic reaction, respectively.

RESULTS AND DISCUSSION

Properties of ZnO-CN(*x*) composites

Fig. 2 shows the XRD patterns of CN, ZnO-CN (*x*) composites prepared from physical mixing method, and the ZnO. As can be seen from Fig. 2 (a), CN showed an intense peak at 2θ of 27.65°, which can be assigned as the graphite-like CN layer. The interlayer distance (*d*) was calculated to be 0.32 nm. The small peak at 2θ of 12.95° showed the hole-to-hole distance of carbon nitride pores with a calculated *d* spacing of 0.68 nm. This result is in good agreement with other literature that also used the urea precursor to prepare the CN (Alim *et al.*, 2015; Jasman *et al.*, 2017a; Jasman *et al.*, 2017b; Lee *et al.*, 2012).

The XRD patterns of ZnO-CN composites are shown in Fig. 2 (b)-(e). The diffraction peaks of the CN still could be observed clearly, but the intensity became lower with the increase of ZnO loading. New diffraction peaks at 2θ of 31.65°, 34.30°, and 36.20° could be detected on ZnO-CN (*1*) sample and the intensity of these peaks also increased with the increase of ZnO loading. As can be observed in Fig. 2 (g), these diffraction peaks could be assigned to the wurtzite ZnO,

according to JCPDS file (JCPDS 89-1397) (Hussin *et al.*, 2015; Hussin *et al.*, 2016; Ma *et al*., 2014; Xie *et al*., 2011).

Fig. 3 reveals the FTIR spectra of CN, ZnO-CN (*x*), and ZnO samples. As shown in Fig. 3 (a), CN showed several peaks due to the vibrations of some bondings occurred between carbon and nitrogen. The band at 810 cm^{-1} showed the characteristic of the triazine unit of CN, while peaks at 1200-1600 cm^{-1} region corresponded to stretching modes of C-N heterocyclics. The absorption peaks at 1340 and 1640 cm^{-1} could be assigned as the stretching modes of C-N and C=N. On the other hand, the broad band observed around 3100–3300 cm^{-1} would be related to the stretching modes of N-H and adsorbed water molecules of O-H groups. All the observed peaks in the FTIR spectrum of CN were similar to the absorption peaks reported previously (Alim *et al.*, 2015; Jasman *et al.*, 2017a; Jasman *et al.*, 2017b), supporting the successful transformation of the urea precursor to the CN.

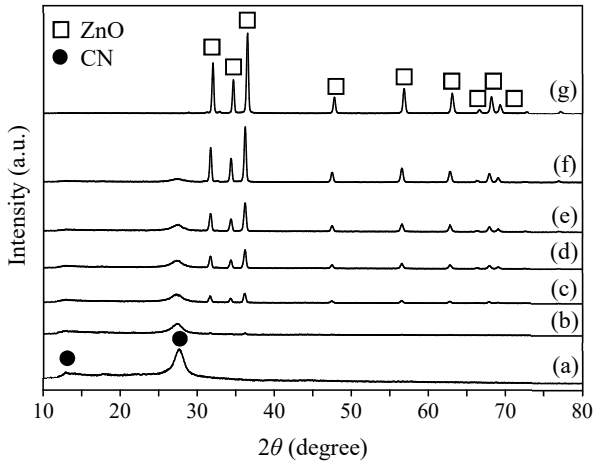

Fig. 2 XRD diffractogram of (a) CN, (b) ZnO-CN (*1*), (c) ZnO-CN (*5*), (d) ZnO-CN (*10*), (e) ZnO-CN (*20*), (f) ZnO-CN (*50*), and (g) ZnO.

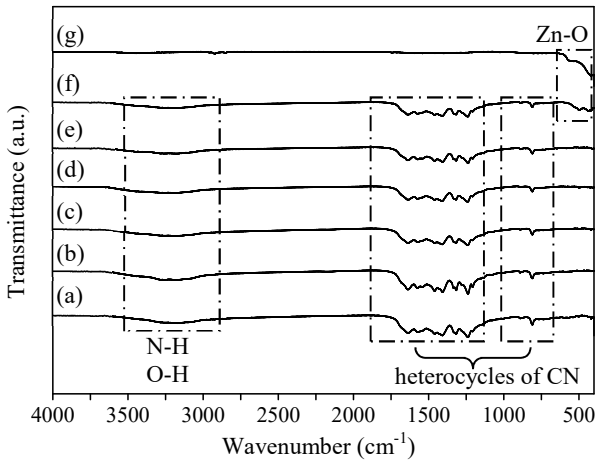

Fig. 3 FTIR spectra of (a) CN, (b) ZnO-CN (*1*), (c) ZnO-CN (*5*), (d) ZnO-CN (*10*), (e) ZnO-CN (*20*), (f) ZnO-CN (*50*), and (g) ZnO.

The FTIR spectra of the prepared ZnO-CN samples are shown in Fig. 3 (b)-(f). Similar to the results of XRD patterns, samples with a high amount of CN showed the absorption peaks of CN as the dominant species. The peaks assigned to the CN decreased with the increase of Zn/C mol ratio. When the mol ratio reached 50 mol%, the peaks related to the CN were completely diminished and only ZnO peak could be observed on the ZnO-CN (*50*) sample. The prepared ZnO showed an intense peak in the range of 400–500 cm^{-1} as depicted in Fig. 3 (g), which was belonged to the Zn-O stretching (Anžlovar *et al*., 2012). The FTIR spectra clearly suggested that the CN and ZnO can be detected on the ZnO-CN (*x*) composite samples, depending on the amount of CN and ZnO.

The optical properties of CN, ZnO and ZnO-CN samples were displayed in Fig. 4. As shown in Fig. 4 (a), the CN sample showed three strong absorption bands around 277, 330 and 370 nm, corresponding to the transitions of N=C groups of aromatic, the 1,3,5-triazine, uncondensed C=O group, and the terminal N-C group of CN, respectively (Alim *et al.*, 2015; Jasman *et al.*, 2017a; Jasman *et al.*, 2017b). It was obvious that the CN sample absorbed visible light based having the absorption edge up to *ca.* 450 nm, suggesting its capability to serve as the visible light-active photocatalyst. For the ZnO-CN (*x*) samples, all samples showed the significant absorption peaks of both CN and ZnO as shown in Fig. 4 (b)-(f). As the ratio of Zn/C increased, the absorption edge of the samples was blue-shifted from *ca.* 450 to *ca.* 380 nm, resembling the characteristic of ZnO. From Fig. 4 (g), the ZnO showed one broad absorption band centered around 320 nm, originated from the electron transfer in the Zn-O. In other words, it could be observed that the presence of the CN would induce the visible absorption of the ZnO. This would be one benefit for the ZnO-CN (*x*) composite photocatalysts.

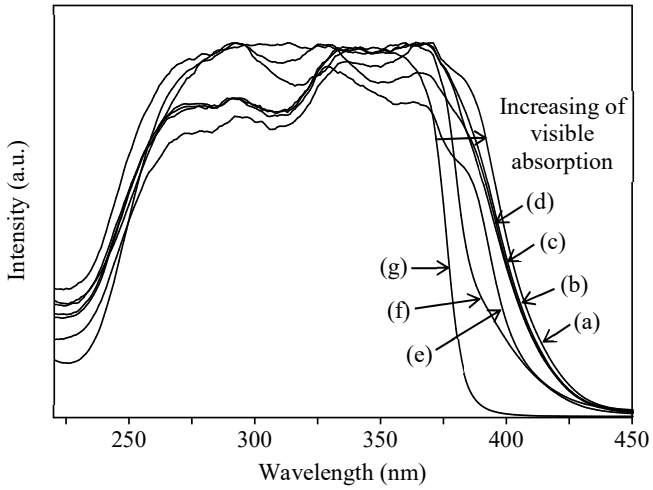

Fig. 4 DR UV-visible spectra of (a) CN, (b) ZnO-CN (*1*), (c) ZnO-CN (*5*), (d) ZnO-CN (*10*), (e) ZnO-CN (*20*), (f) ZnO-CN (*50*), and (g) ZnO.

The BET specific surface areas of all samples are listed in Table 1. The CN possesses a specific surface area of 70 $m^2 g^{-1}$ (Entry 1). As for the ZnO-CN (*x*) samples, it was observed that addition of ZnO did not contribute to the enhancement of surface area, but as the Zn/C mol ratio increased, the surface area decreased consistently from 70 to 26 $m^2 g^{-1}$ (Entries 2-6). This was reasonable since ZnO might block the surface of the CN. Moreover, the ZnO showed a low surface area, which was around 7 $m^2 g^{-1}$ (Entry 7).

Table 1 BET specific surface area of CN, ZnO-CN (*x*) composites, and ZnO.

Entry	Sample	BET specific surface area ($m^2 g^{-1}$)
1	CN	70
2	ZnO-CN (*1*)	63
3	ZnO-CN (*5*)	56
4	ZnO-CN (*10*)	51
5	ZnO-CN (*20*)	42
6	ZnO-CN (*50*)	26
7	ZnO	7

The effect of ZnO addition to the emission of the CN was investigated by recording the emission spectra of the CN and the ZnO-CN (*x*) samples at the excitation wavelength of CN, which was 273 nm. The excitation wavelength of 273 nm was correlated to the N=C groups of aromatic 1,3,5-triazine (Alim *et al.*, 2015; Jasman *et al.*, 2017a; Jasman *et al.*, 2017b; Sam *et al*., 2014) and was used to represent the close interactions between the ZnO and the CN. As shown in Fig. 5, the CN gave two emission sites at 445 and 460 nm.

The emission intensity of the CN decreased with the presence of ZnO. The decrease in the intensity was more pronounced with the higher ratio of Zn/C, clearly suggesting that there were close interactions between the emission sites of the CN and the added ZnO. Since the emission spectrum is closely associated with the charge recombination, low emission intensity would imply the low recombination. Therefore, it could be proposed that the addition of ZnO could suppress the charge recombination of the CN. In addition to the charge recombination, the addition of high loading amount of ZnO might also decrease the emission intensity of the CN due to the blocking of the emission sites by the ZnO.

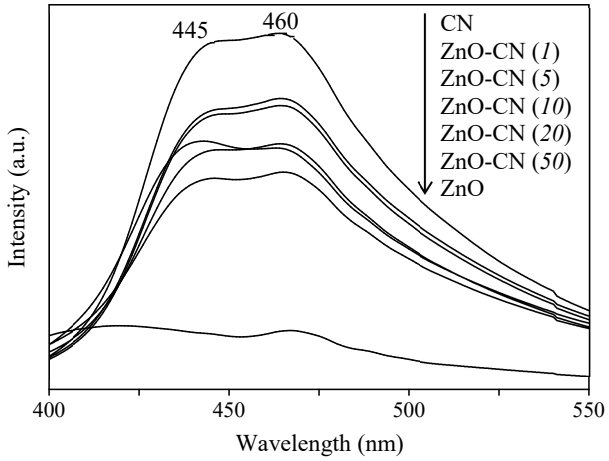

Fig. 5 Fluorescence emission spectra of CN and ZnO-CN (*x*) composites.

Evaluation of photocatalytic activity of ZnO-CN (*x*) composites

The activity of CN, the ZnO-CN (*x*) composites, and the ZnO was evaluated for the photocatalytic phenol degradation. Each reaction was conducted for 5 h under UV or visible light irradiation and the results are shown in Table 2. Under UV light irradiation, CN achieved 17.0% phenol degradation, while the ZnO was able to degrade phenol at 50.4%. As for the ZnO-CN (*x*) composites, the addition of ZnO remarkably enhanced the activity of the CN from 17% to 45% when the ratio of Zn/C was 10 mol% and above. The activity of these ZnO-CN composites was almost 2.6 times better than the individual CN. This result clearly proved that the addition of ZnO promoted the UV light activity of the CN in the composites.

Table 2 Photocatalytic degradation of phenol under UV and visible light irradiation over CN, ZnO-CN (*x*) composites, and ZnO.

Sample	Percentage of phenol degradation under UV light (%)	Percentage of phenol degradation under visible light (%)
CN	17	33
ZnO-CN (*1*)	20	38
ZnO-CN (*5*)	39	36
ZnO-CN (*10*)	45	34
ZnO-CN (*20*)	45	34
ZnO-CN (*50*)	45	34
ZnO	50	15

On the other hand, under visible light irradiation, the CN showed 33% phenol degradation, while the ZnO achieved 15% phenol degradation. When a small amount of ZnO (1 mol%) was added to the CN, the activity increased from 33% to 38%. Unfortunately, when the ZnO content was more than 1 mol%, the activity was found to be gradually decreased with the increase of the Zn/C ratio. It is worth noted that the ZnO-CN (*1*) showed a better photocatalytic activity, higher than both the bare CN and the bare ZnO. The activity of the ZnO-CN (*1*) composite was almost 1.15 and 2.5 times higher than the activity of the bare CN and the bare ZnO, respectively. This result clearly showed that there was a synergic effect between the small amount of ZnO and the CN as supported by the fluorescence study, where the emission intensity of the CN was reduced with the addition of ZnO. However, it was observed that the composite with the lowest emission intensity did not give the highest activity under visible light irradiation. As aforementioned above, the reduced emission intensity was also caused by the blockage of the CN by the ZnO. This result showed that the optimum small amount of ZnO was important to both maintain the light absorption of the CN and reduce the electron-hole recombination.

The small amount of ZnO could trap the electrons of the CN, and thus, inhibited the electron-hole recombination process in the CN sample. The less electron-hole recombination would be the key factor to get the improvement of photocatalytic activity toward the degradation of phenol. Moreover, a small amount of ZnO could decrease the charge transfer resistance, which improved the photocatalytic process toward degradation of phenol (Hussin *et al.*, 2016). Therefore, the ZnO-CN (*1*) sample showed the highest activity among the composite samples. From the point of view of ZnO, the 2.5 times higher activity obtained on the ZnO-CN (*x*) composites strongly suggested that the presence of the CN became the important parameter to achieve high activity under visible light irradiation. The improved photocatalytic degradation over the ZnO-CN (*x*) composites under UV and visible light irradiation is summarized in Fig. 6.

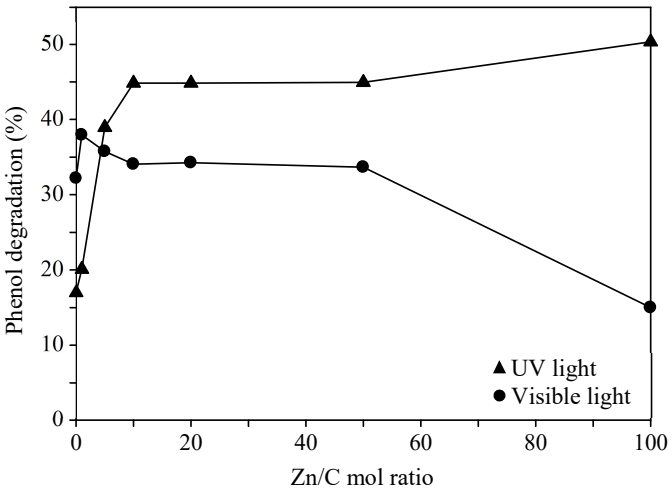

Fig. 6 Phenol degradation over CN, ZnO-CN (*x*) composites, and ZnO under UV and visible light irradiation.

Comparison to the activity of the ZnO-CN composites prepared by the impregnation of ZnO onto the CN (Hussin *et al.*, 2016), the current composites prepared by a simple physical mixing method gave a similar level of activity under visible light irradiation. This result suggested that as long as the close contacts between the ZnO and the CN could be achieved, the high activity could be expected and the physical mixing method could provide such synergic effect. Moreover, since physical mixing was carried out at room temperature, this method could more retain the CN structure even at high ZnO/C ratio. On the other hand, since the impregnation method was carried out at high temperature (550 °C), the composites showed more reduced activity with the increase of Zn/C ratio due to a more reduced CN structure as evidenced by XRD and FTIR spectroscopies (Hussin *et al.*, 2016). As has been reported previously, the crystallinity of ZnO is an important parameter to obtain high activity for degradation of phenol (Hussin, *et al.*, 2015). Therefore, in addition to the ZnO crystallinity, this study showed that the remained intact structure of the CN was also one significant factor in designing the active ZnO-CN composite photocatalysts.

CONCLUSION

The ZnO-CN (*x*) samples were successfully prepared via the physical mixing method. The addition of ZnO helped to improve the

activity of the CN both under UV and visible light irradiation. The ZnO-CN composites with the optimum amount of Zn/C ratio, which were 10 and 1 mol%, set the highest activity with 2.6 and 1.15 times better than the CN under UV and visible light, respectively. The improved photocatalytic efficiency on ZnO-CN composite photocatalysts was caused by the synergic effect between ZnO and CN. The ZnO would boost the separation efficiency of photogenerated electrons on the CN and the CN would extend the absorption of the ZnO in the visible light region.

ACKNOWLEDGEMENTS

This work was financially supported by the Ministry of Higher Education (MOHE, Malaysia) and Universiti Teknologi Malaysia (UTM, Malaysia) through the Research University Grant (Tier 1, cost center code: Q.J130000.2509.06H66). F.H acknowledges the support of UTM through the Zamalah scholarship.

REFERENCES

Alim, N. S., Lintang, H. O., Yuliati, L. 2015. Fabricated metal-free carbon nitride characterizations for fluorescence chemical sensor of nitrate ions. *J. Teknol.* 76, 13, 1–6.

Ansari, S. A., Husain, Q., Qayyum, S., Azam, A. 2011a. Designing and surface modification of zinc oxide nanoparticles for biomedical applications. *Food Chem. Toxicol.* 49, 9, 2107–2115.

Ansari, M. B., Min, B.-H., Mo, Y.-H., Park, S.-E. 2011b. CO_2 activation and promotional effect in the oxidation of cyclic olefins over mesoporous carbon nitrides. *Green Chem*. 13, 6, 1416–1421.

Arya, S. K., Saha, S., Ramirez-Vick, J. E., Gupta, V., Bhansali, S., Singh, S. P. (2012). Recent advances in ZnO nanostructures and thin films for biosensor applications: Review. *Anal. Chim. Acta* 737, 6, 1–21.

Behnajady, M. A., Modirshahla, N., Hamzavi, R. 2006. Kinetic study on photocatalytic degradation of C.I. Acid Yellow 23 by ZnO photocatalyst. *J. Hazard. Mater.* 133, 1–3, 226–232.

Cauda, V., Pugliese, D., Garino, N., Sacco, A., Bianco, S., Bella, F., Lamberti, A., Gerbaldi, C. 2014. Multi-functional energy conversion and storage electrodes using flower-like zinc oxide nanostructures. *Energy* 65, 639–646.

Chekir, N., Benhabiles, O., Tassalit, D., Laoufi, N. A., Bentahar, F. 2016. Photocatalytic degradation of methylene blue in aqueous suspensions using TiO_2 and ZnO. *Desalin. Water Treat.* 57, 13, 6141–6147.

Chen, C.-C., Fan, H.-J., Jan, J.-L. 2008a. Degradation pathways and efficiencies of Acid Blue 1 by photocatalytic reaction with ZnO nanopowder. *J. Phys. Chem. C.* 112, 31, 11962–11972.

Chen, D., Wang, Z., Ren, T., Ding, H., Yao, W., Zong, R., Zhu, Y. 2014. Influence of defects on the photocatalytic activity of ZnO. *J. Phy. Chem. C.* 118, 28, 15300–15307.

Chen, L.-C., Tu, Y.-J., Wang, Y.-S., Kan, R.-S., Huang, C.-M. 2008b. Characterization and photoreactivity of N-, S-, and C-Doped ZnO under UV and visible light illumination. *J. Photochem. Photobiol. A.* 199, 2–3, 170–178.

Djurišić, A. B., Ng, A. M. C., Chen, X. Y. 2010. ZnO nanostructures for optoelectronics: Material properties and device applications. *Prog. in Quantum Electron.* 34, 4, 191–259.

Fu, J., Chang, B., Tian, Y., Xi, F., Dong, X. 2013. Novel C_3N_4–CdS composite photocatalysts with organic–inorganic heterojunctions: *in situ* synthesis, exceptional activity, high stability and photocatalytic mechanism. *J. Mater. Chem. A*. 1, 9, 3083–3090.

Huang, J., Yin, Z., Zheng, Q. 2011. Applications of ZnO in organic and hybrid solar cells. *Energy Environ. Sci.* 4, 10, 3861–3877.

Hussin, F., Lintang, H. O., Lee, S. L., Yuliati, L. 2015. Preparation of highly active zinc oxide for photocatalytic removal of phenol: Direct calcination versus co-precipitation method. *Mal. J. Fund. Appl. Sci.* 11, 3, 134–138.

Hussin, F., Lintang, H. O., Yuliati, L. 2016, Enhanced activity of C_3N_4 with addition of ZnO for photocatalytic removal of phenol under visible light. *Mal. J. Anal. Sci.* 20, 1, 102–110.

Grätzel M. 2001, Photoelectrochemical cells, *Nature* 414, 338–344.

Jasman, S. M., Lintang, H. O., Yuliati, L. 2017a. Enhanced detection of nitrite ions over copper acetylacetonate/polymeric carbon nitride composites. *Macromol. Symp*. 371, 84–93.

Jasman, S. M., Lintang, H. O., Lee, S. L., Yuliati, L. 2017b. Copper modified carbon nitride as fluorescence sensor for nitrate ions. *Mal. J. Anal. Sci*. 21, 6, 1316–1326.

Jiang, J., Zhang, X., Sun, P., Zhang, L. 2011. ZnO/BiOI heterostructures : Photoinduced charge-transfer property and enhanced visible-light photocatalytic activity. *J. Phys. Chem. C.* 115, 42, 20555–20564.

Kong, J.-Z., Li, A.-D., Zhai, H.-F., Gong, Y.-P., Li, H., Wu, D. 2009. Preparation, characterization of the Ta-Doped ZnO nanoparticles and their photocatalytic activity under visible-light illumination. *J. Solid State Chem.* 182, 8, 2061–2067.

Lee, S. C., Lintang, H. O., Yuliati, L. 2012. A urea precursor to synthesize carbon nitride with mesoporosity for enhanced activity in the photocatalytic removal of phenol. *Chem. Asian J.* 7, 9, 2139–2144.

Lee, S. C., Chew, W. S., Lintang, H. O., Yuliati, L. Photocatalytic removal of cyclohexane on visible light-driven gallium oxide/carbon nitride composites prepared by impregnation method. *Mal. J. Fund. Appl. Sci.* 11, 3, 98–101.

Li, L., Zhai, T., Bando, Y., Golberg, D. 2012. Recent progress of one-dimensional ZnO nanostructured solar cells. *Nano Energy*, 1, 1, 91–106.

Li, Y., Zhou, X., Hu, X., Zhao, X., Fang, P. 2009. Formation of surface complex leading to efficient visible photocatalytic activity and improvement of photostability of ZnO. *J. Phys. Chem. C.* 113, 36, 16188–16192.

Logothetidis, S., Laskarakis, A., Kassavetis, S., Lousinian, S., Gravalidis, C., Kiriakidis, G. 2008. Optical and structural properties of ZnO for transparent electronics. *Thin Solid Films*, 516, 7, 1345–1349.

Lorenz, H., Friedrich, M., Armbrüster, M., Klötzer, B., Penner, S. 2013. ZnO is a CO_2-selective steam reforming catalyst. *J. Catal.*, 297, 151–154.

Ma, T. Y., Dai, S., Jaroniec, M., Qiao, S. Z. 2014. Graphitic carbon nitride nanosheet–carbon nanotube three-dimensional porous composites as high-performance oxygen evolution electrocatalysts. *Angew. Chem. Int. Ed.* 53, 28, 7281–7285.

Olad, A., Nosrati, R. 2012. Preparation, characterization, and photocatalytic activity of polyaniline/ZnO nanocomposite. *Res. Chem. Intermed.* 38, 2, 323–336.

Qiu, R., Zhang, D., Mo, Y., Song, L., Brewer, E., Huang, X., Xiong, Y. 2008. Photocatalytic activity of polymer-modified ZnO under visible light irradiation. *J. Hazard. Mater.* 156, 1–3, 80–85.

Sabbaghan, M. and Ghalaei, A. 2014. Catalyst application of ZnO nanostructures in solvent free synthesis of polysubstituted pyrroles. *J. Mol. Liq*. 193, 116–122.

Saikia, L., Bhuyan, D., Saikia, M., Malakar, B., Dutta, D. K., Sengupta, P. 2015. Photocatalytic performance of ZnO nanomaterials for self sensitized degradation of malachite green dye under solar light. *Appl. Catal. A* 490, 42–49.

Sam, M.S., Lintang, H.O., Sanagi, M.M., Lee, S.L., Yuliati, L. 2014. Mesoporous carbon nitride for adsorption and fluorescence sensor of N-nitrosopyrrolidine. *Spectrochim. Acta, Part A*. 124, 357–364.

Saravanan, R., Karthikeyan, S., Gupta, V. K., Sekaran, G., Narayanan, V., Stephen, A. 2013. Enhanced photocatalytic activity of ZnO/CuO nanocomposite for the degradation of textile dye on visible light illumination. *Mater. Sci. Eng. C*. 33, 1, 91–98.

Saravanan, R., Shankar, H., Prakash, T., Narayanan, V., Stephen, A. 2011. ZnO/CdO composite nanorods for photocatalytic degradation of methylene blue under visible light. *Mater. Chem. Phys*. 125, 1–2, 277–280.

Velmurugan, R., Swaminathan, M. 2011. An efficient nanostructured ZnO for dye sensitized degradation of reactive Red 120 Dye under solar light. *Sol. Energy Mater. Sol. Cells* 95, 3, 942–950.

Xie, J., Wang, H., Duan, M., Zhang, L. 2011. Synthesis and photocatalysis properties of ZnO structures with different morphologies *via* hydrothermal method. *Appl. Surf. Sci*. 257, 15, 6358–6363.

Yan, H., Yang, H. 2011. TiO_2-g-C_3N_4 composite materials for photocatalytic H_2 evolution under visible light irradiation. *J. Alloys Compd.* 509, 4, L26–L29.

Yang, G. C. C., Chan, S. W. 2009. Photocatalytic reduction of chromium(VI) in aqueous solution using dye-sensitized nanoscale ZnO under visible light irradiation. *J. Nanopart. Res*. 11, 1, 221–230.

Yuliati, L., Abd Kadir, A. H., Lee, S. L., Lintang, H. O. 2017. Fluorescence quenching on mesoporous carbon nitride by phenol and aniline. *Mal. J. Anal. Sci.* 21, 6, 1342–1351.

Zhang, D., Zeng, F. 2012. Visible light-activated cadmium-doped ZnO nanostructured photocatalyst for the treatment of methylene blue dye. *J. Mater. Sci.* 47, 5, 2155–2161.

Zhang, H., Zuo, X., Tang, H., Li, G., Zhou, Z., 2015. Origin of photoactivity in graphitic carbon nitride and strategies for enhancement of photocatalytic efficiency: insights from first-principles computations. *Phys. Chem. Chem. Phys.* 17, 9, 6280–6288.